Journal of Chromatography A 1704 (2023) 464131

Contents lists available at ScienceDirect

Journal of Chromatography A

journal homepage: www.elsevier.com/locate/chroma

Evolution of anthocyanin content during grape ripening and characterization of the phenolic profile of the resulting wine by comprehensive two-dimensional liquid chromatography

Laura Oliveira Lago[a,1], Pawel Swit[b,1], Mairon Moura da Silva[c], Aline Telles Biasoto Marques[d], Juliane Welke[a], Lidia Montero[e], Miguel Herrero[e,*]

[a] Institute of Food Science and Technology (ICTA), Federal University of Rio Grande do Sul (UFRGS), Zip Code 91501970, Porto Alegre, Brazil
[b] Institute of Chemistry, Faculty of Science and Technology, University of Silesia in Katowice, Szkolna 9, 40-006 Katowice, Poland
[c] Department of Agronomy, Academic Unit of Garanhuns, Federal Rural University of Pernambuco (UAG-UFRPE), Garanhuns, PE, Brazil
[d] Embrapa Meio Ambiente, Zip Code 13918110, Jaguariúna, SP, Brazil
[e] Laboratory of Foodomics, Institute of Food Science Research - CIAL (CSIC-UAM), Nicolás Cabrera 9, 28049 Madrid, Spain

ARTICLE INFO

Article history:
Received 17 March 2023
Revised 17 May 2023
Accepted 3 June 2023
Available online 4 June 2023

Keywords:
Phenolic compounds
Grape
Wine
Two-dimensional liquid chromatography
LC × LC

ABSTRACT

The typical phenolic profile in grapes is characterized by its complexity both in terms of number of diverse chemical structures and their variation during ripening. Besides, the specific phenolic composition of grapes directly influences the presence of those components in the resulting wine. In this contribution, a new method based on the application of comprehensive two-dimensional liquid chromatography coupled to a diode array detector and tandem mass spectrometry has been developed to obtain the typical phenolic profile of Malbec grapes cultivated in Brazil. Moreover, the method has been demonstrated to be useful to study how the phenolic composition in grapes evolved during a 10-week ripening period. Main detected compounds in grapes and in the wine derived from them were anthocyanins, although a good number of polymeric flavan-3-ols were also tentatively identified, among other compounds. Results show how the amount of anthocyanins present in grapes was increased during ripening up to 5–6 weeks and then decreased towards week 9. The two-dimensional approach applied was demonstrated to be useful for the characterization of the complex phenolic profile of these samples, involving more than 40 different structures and has the potential to be further applied to the study of this important fraction is different grapes and wines systematically.

1. Introduction

Phenolic compounds are a group of natural bioactive molecules found mainly in vegetables and fruits, including grapes and their by-products such as wine [1]. They are produced in grapes in response to environmental stress, like predation, attack by microorganisms, UV light levels and water deficit. Their composition and content in wine is greatly influenced by grape variety and maturity stage, technological practices to which grapes are exposed, type of yeast and bacteria used in the alcoholic and malolactic fermentation, respectively, and contact with solid parts of the grape during maceration [2–4].

Polyphenols are essential in the quality of wine, especially red ones, contributing to sensory properties (color, flavor, astringency and bitterness). Besides, they have been described to have antioxidant, anti-inflammatory, cardioprotective and anti-hypertensive activity and positive effects on human microbiota composition and functionality. Thus, different previously presented studies have been focused on the determination of these compounds [3,5,6].

They are characterized by having an enormous structural variability, ranging from simple phenolic molecules to highly polymerized compounds, and are mostly found in conjugated forms with mono- and polysaccharides, that can be linked to different positions within the polyphenolic structure. This usually makes the profiling of these compounds a laborious task [3,7]. The analytical approach most-frequently adopted to identify these bioactive

* Corresponding author.
E-mail address: m.herrero@csic.es (M. Herrero).
[1] These authors contributed equally to this work.

https://doi.org/10.1016/j.chroma.2023.464131

compounds is liquid chromatography (LC). Nevertheless, if the polyphenolic content of the analyzed sample is very complex, the typically used one-dimensional LC (1D-LC) might not be sufficient for obtaining enough resolution [8,9]. On this matter, the utilization of multidimensional approaches, such as comprehensive two-dimensional liquid chromatography (LC × LC), considerably enhances the separation potential since it takes advantage of the combination of two independent separation mechanisms to effectively boost the available resolving power as well as to produce a powerful increase on peak capacity [10]. One of the key features of this technique is that the whole sample is analyzed through two separation mechanisms (dimensions). Consequently, compounds that are not resolved in a single separation may be further separated using a second separation. Due to the excellent resolving power provided, LC × LC has been demonstrated as a really useful tool for different purposes in food analysis [11–13]. As grapes and wines are considered very complex samples in terms of polyphenols composition, different works have explored the possibility of using different LC × LC coupling for their analysis, including for the identification of polyphenols in wines [14,15], grapes [16], grape juices [17] and winemaking by-products, such as seeds [18] or grapevine canes [19]. Among the different couplings of separations mechanisms that can be combined, the use of hydrophilic interaction chromatography (HILIC) and reversed phase (RP) conditions in the first (^{1}D) and second (^{2}D) dimensions, respectively, has shown an excellent potential for polyphenols analysis [20,21]. This coupling is characterized by a high degree of orthogonality, as separations in the two dimensions are based on non-correlated mechanisms. However, important issues make its application challenging, mainly the solvent strength mismatch produced between the solvents used as mobile phases in the ^{1}D and those used in the ^{2}D [22]. In this regard, different modulation procedures have been proposed to limit this problem and improve the peak shapes and resolution in the ^{2}D separations. Among them, the use of focusing modulation or the use of a dilution step of the ^{1}D effluent before being injected in the ^{2}D have been shown as good strategies to reduce the solvent incompatibility effect [22,23].

In this context, the aim of this article is to develop a new LC × LC method that combines a HILIC separation in the ^{1}D with a RP-based separation in the ^{2}D coupled to diode array detector (DAD) and tandem mass spectrometry (MS/MS) to characterize the anthocyanin profile of Malbec grapes with different degrees of ripeness and the phenolic profile of wine produced from them to study the composition and evolution of polyphenols during grape maturation as well as the final composition after winemaking. To the best of our knowledge, this is the first report in which a dedicated LC × LC method is applied to study the evolution of secondary metabolites over time in foods.

2. Materials and methods

2.1. Samples and chemicals

Grape (*Vitis vinifera* L.) samples from the variety Malbec were collected from a vineyard from Garanhuns (Pernambuco, Brazil) between December 2021 and February 2022. This cultivar was chosen because it stood out in terms of aptitude and productivity in this region. Grape samples were collected weekly (during 10 weeks) from the phenological stage number 35 of the vine (beginning of ripening; berries beginning to color and softening) [24], totalizing 10 samples: W1, W2, W3, W4, W5, W6, W7, W8, W9 and W10.

The wine was produced with grapes harvested at W9, as this is the usual practice adopted by wineries in this Brazilian region. The red wine was prepared in the Oenology Laboratory of Embrapa Semiárido in the city of Petrolina, Pernambuco. Potassium metabisulfite, commercial yeast *Saccharomyces cereviseae* var. bayanus Maurivin PDM (0.20 – 0.30 g L^{-1}), Gesferm® ammonium phosphate fermentation activator (around 0.20 g L^{-1}) and Everzym color® pectinolytic enzyme (0.01 - 0.03 g L^{-1}) were used as oenological adjuvants. After destemming and crushing the grapes, alcoholic fermentation and solid-liquid maceration were carried out at 24 ± 2 °C. Subsequently, spontaneous malolactic fermentation was performed at 17 ± 1 °C, until the complete transformation of malic acid into lactic acid, evidenced by paper chromatography (around 30 days), and cold tartaric stabilization (0 °C) for ten days, and with the addition of 0.4 g L^{-1} of Stabigum® (E414 Gum arabic + E353 metatartaric acid). Bottling was carried out in dark bottles of 750 mL, with prior correction of the free sulfur dioxide content to 50 mg L^{-1}. The bottles were stored for 30 days in a horizontal position in a wine cellar at 16 ± 1 °C and humidity around 60% for the aging of the wine in the bottle.

HPLC grade methanol, acetic and formic acid were purchased from VWR Chemicals (France). Acetonitrile (LC grade) was supplied by Carlo Erba Reagents (France). Water employed was Milli-Q grade obtained from a Millipore system (Billerica, MA).

2.2. Extraction of phenolic compounds from grape and wine

The phenolic compounds were extracted according to a previously published method [25], with some modifications. Grape samples were lyophilized (Liotop® L101, Vitória, Brazil) at -58 ± 2 °C and 6.7 ± 1 Pa for around 96 h to obtain samples with moisture of 1.5 ± 0.2%. The extraction of phenolic compounds from the lyophilized samples W1-W10 (0.5 g in 50 mL falcon tubes) was performed using 5 mL of a methanol:water solution (8:2, *v/v*) acidified with 0.35% formic acid, vortexing for 3 min followed by centrifugation (3000 rpm, 4 °C, 5 min) on a Rotina 380R centrifuge (Hettich, Tuttlingen, Germany). The described procedure was repeated 5 times. Supernatants were pooled and evaporated with nitrogen. The sample was reconstituted with 1 mL of methanol. The extracts were then filtered through a nylon syringe filter (0.45 µm) and placed in 3 mL HPLC vials. Extraction procedure was performed in triplicate. The phenolic compound extraction from wine was carried out by using 5 mL of the sample and 5 mL of a methanol:water solution (8:2, *v/v*) acidified with 0.35% formic acid. The mixture was vortexed for 3 min and evaporated with nitrogen. The sample was reconstituted with 1 mL of methanol. Extraction procedure was performed in triplicate.

2.3. LC × LC analyses

2.3.1. Instrumentation

LC × LC instrumentation consisted of an Agilent 1200 series liquid chromatograph (Agilent Technologies, Santa Clara, CA) equipped with an autosampler. Additionally, a LC pump (Agilent 1290 Infinity) was coupled to perform the second dimension (^{2}D) separation. ^{1}D and ^{2}D were connected by an electronically-controlled two-position ten-port switching valve (Rheodyne, Rohnert Park, CA, USA) acting as a modulator equipped with two identical 50 μL or 100 μL injection loops. Modulation time of the switching valve was 1 min or 1.5 min as indicated below. For the introduction of the make-up flow when necessary, an additional Agilent 1200 series pump controlled using a 1200 Instant Pilot (Agilent) was employed. A diode array detector (DAD) was coupled after the second dimension in order to register every ^{2}D analysis. Signals at 280, 254 and 550 nm were monitored and UV–Vis spectra from 190 to 550 nm were registered using a sampling rate of 20 Hz. Besides, an Agilent 6320 ion trap mass spectrometer (MS) equipped with an electrospray interface working under positive

ionization mode was coupled in series using the following conditions: dry temperature, 350 °C; dry gas flow rate, 12 L min^{-1}; nebulization pressure, 345 Pa; mass range, *m/z* 90–1200 Da; ultra scan mode (26,000 *m/z*/s). Auto MS(n) was performed for acquiring tandem MS/MS spectra. The flow eluting from the ^{2}D column was split before entering MS instrument to ca. 0.7 mL min^{-1}. The LC data were elaborated and visualized using LC Image software (version 1.0, Zoex Corp., Houston, TX). For method optimization, different columns were tested in the ^{1}D and in the ^{2}D. The used columns, as their main characteristics are included in Table S1.

2.3.2. LC × LC separation conditions

The final LC × LC separation conditions were obtained after optimization, as described below, involving the following conditions:

i) ^{1}D separation: ZIC–HILIC column (150 × 1 mm, 3.5 µm, Merck, Darmstadt, Germany) eluted using acetonitrile (A) and 10 mM ammonium acetate, pH 5 (B) at 25 µL min^{-1} applying the following gradient: 0 min, 5% B; 20 min, 25% B; 30 min, 30% B; 45 min, 35% B; 50 min, 40% B; 80 min, 55% B; 85 min, 5% B; 100 min, 5% B. In all cases, the injection volume was 10 μL.

ii) ^{2}D separation: C18 column (Ascentis Express C18, 50 × 4.6 mm, 2.7 μm, Supelco, Bellefonte, CA) eluted using water (0.1% formic acid, A) and acetonitrile (B) at 3.0 mL min^{-1} with the following 1.5 min repetitive gradients: 0 min, 5% B; 0.3 min, 5% B; 0.8 min, 30% B; 0.9 min, 40% B; 1 min, 90% B; 1.2 min, 90% B; 1.21 min, 5% B. This gradient was repeated during the whole LC × LC analysis time. To match the duration of each ^{2}D separation, the modulation time set for the switching valve actuation was 1.5 min.

Moreover, an additional make-up flow was introduced to reduce the relative solvent strength at the exit of the ^{1}D using a T-piece at a flow rate of 75 µL min^{-1}. The make-up flow was composed of water. When the make-up flow was employed, the final separation conditions used in the ^{2}D involved the same column and mobile phases as above stated, although the elution conditions were adjusted as follows: 0 min, 5% B; 0.1 min, 15% B; 0.3 min, 20% B; 0.8 min, 35% B; 0.81 min, 5% B; using a flow rate of 2.5 mL min^{-1}. This gradient was repeated during the whole LC × LC analysis time. To match the duration of each ^{2}D separation, the modulation time set for the switching valve actuation was 1.0 min. Besides, the sampling loops employed under this set-up had an inner volume of 100 μL.

Other columns tested in both dimensions are described in Section 3.

2.3.3. Theory, peak capacity, orthogonality

To estimate the main figures-of-merit of the developed 2DLC approaches, different calculations were carried out, specifically to provide values or peak capacity and orthogonality.

Peak capacity (n_c) was calculated for each dimension starting from the basic equation shown below (1):

$$n_c = 1 + \frac{t_G}{\bar{w}} \quad (1)$$

where t_G is the gradient time and $\overline{w}$ is the average peak width. For both dimensions, the average peak width was obtained from no less than 10 representative peaks selected along the analyses. Peak broadening factor $<\beta>$ has been proposed to correct ^{1}D peak capacity in LC × LC systems, so that the potential deleterious effect of undersampling of the ^{1}D effluent is considered. This parameter was calculated as follows:

$$^1n_{c,\,corrected} = \frac{^1n_c}{\sqrt{1 + 0.21\left(\frac{t_S}{^1\sigma}\right)^2}} \quad (2)$$

where t_s is the sampling time and $^1\sigma$ is the average width of ^{1}D peaks as standard deviation in time units before modulation. With this information, the overall LC × LC peak capacity was calculated as follows:

$$^{2D}n_{c,\,theoretical} = {}^1n_c \times {}^2n_c \quad (3)$$

This eq. (3) simply follows the so-called product rule. To have a more realistic value, and to correct possible effects from modulation and undersampling, practical peak capacity was calculated as follows (eq. (4)):

$$^{2D}n_{c,\,practical} = \frac{^1n_c \times {}^2n_c}{\sqrt{1 + 3.35 \times \left(\frac{^2t_c \times {}^1n_c}{^1t_G}\right)^2}} \quad (4)$$

Where ^2t_c is the ^{2}D separation time cycle (equal to the modulation time). It has to be noted, that this calculation already considers $\langle\beta\rangle$.

To estimate the orthogonality (A_0) degree of the system, the approach based on asterisk equations was followed [26]. Briefly, this method considers the spread of peaks along the four imaginary lines crossing the 2D space forming an asterisk. More practical details can be found elsewhere [19,26].

2.4. Conventional one-dimensional LC

Conventional one-dimensional LC analyses of the grape and wine samples were performed using an Agilent 1200 series liquid chromatograph (Agilent Technologies, Santa Clara, CA) equipped with an autosampler. The method used was based on a previously reported [27], with some modifications. Briefly, a C18 column (column (150 × 2.1, 3 µm, Phenomenex, Germany) was employed. The mobiles phases employed consisted of water (0.1% formic acid, solvent A) and acetonitrile (0.1% formic acid, solvent B), eluted at 0.2 mL min^{-1} using the following gradient: 0 min, 5% B; 5 min, 15% B; 30 min, 50% B; 35 min, 65% B; 38 min, 100% B. The detection was performed using a DAD, recording the signals at 280, 490 and 550 nm and the injection volume was 10 µL.

3. Results and discussion

3.1. Optimization of separation

Under 1DLC conditions, the separation of phenolic compounds is commonly performed in reversed phase mode using C18 columns [27]. In order to evaluate the potential of conventional 1DLC and the eventual need for LC × LC for the separation of these complex samples, both, the wine and a grape sample (W9) were analyzed using a conventional C18 column. As can be observed in Fig. S1, the complexity of the phenolic compounds pattern present in the samples did not allow obtaining a complete separation of the compounds. Both chromatograms were characterized by the presence of large humps containing many coeluted compounds without baseline separation. This fact clearly pointed to the need for LC x LC separations.

In this context, an online comprehensive 2DLC method, as orthogonal as possible was targeted for the analysis of the grape and wine samples included in the present study. The final aim was to find the analytical conditions allowing a proper separation of the phenolic fraction present in these complex samples. Red grape and wine phenols are believed to be composed of a heterogeneous mixture of phenolic acids, flavan-3-ols, flavonols and anthocyanins [28]. For this reason, to obtain the complete phenolic profile of these samples, analytical methods with sufficient resolving power are needed, as previously demonstrated. In this regard, the use of LC × LC combining the use of a HILIC-based separation in the ^{1}D

together with a C18 column in the ^{2}D has already been shown to provide appropriate levels of separation power and it is characterized by a high degree of orthogonality [21,20]. Consequently, this combination was the one selected for the characterization of grapes and wine polyphenols in the present research.

Initially, the optimization of the separation conditions in each dimension was carried out individually. To do that, a selected grape sample (harvested at week 10, W10) was used as model sample and injected using conventional one-dimensional LC emulating the conditions that should be employed later on in the 2DLC method. Table S1 shows the columns screened for the ^{1}D separation. The aim of this screening was to test the capabilities of different stationary phases for the separation of the polyphenols, including diol, ZIC–HILIC, and silica particles. For each column, a separate optimization was performed. Fig. S2 shows the chromatograms obtained after optimization for each tested column. As can be observed, the best results were obtained using the ZIC–HILIC column as it provided the best compromise between sample distribution (number of separated peaks and wide of those) and analysis time. The other tested columns also provided separations that could be suitable for the LC × LC method, as the sample was widely distributed, although at the expense of significantly longer analysis times. Besides, the sample was just separated in 2–3 big humps, increasing the chance for coelutions in the final 2DLC method. These separations using diol and silica stationary phases could not be further improved, even after thorough optimization. Consequently, the ZIC–HILC column was selected for the LC × LC analyses.

An important aspect considered is that the minimum possible flow rate providing a good distribution along the separation space for a given reasonable analysis time was considered optimum. For the ^{2}D, and based on our previous experience, two stationary phases (C18 and PFP) were tested, both packed inside a short column and in the form of partially porous particles. The use of this type of particles allows a good resolution with lower backpressures produced. For the optimization, a total analysis time of 1.5 min was established as target time to allow the separation and re-conditioning of the column using very high flow rates (> 2.0 mL min^{-1}). In Fig. S3, a comparison of the performance of the two tested columns under optimum separation conditions is shown. As can be observed, the C18 column provided an increased separation power with respect to the PFP column, showing a significantly higher number of separated peaks. In this latter case, an increase in the flow rate employed with the aim to decrease the total analysis time did not improve the separation of the two big humps obtained.

Although the conditions shown in Fig. S3 are not actually produced under a 2DLC analysis, bearing in mind that here the whole sample is being injected, the obtained separations provide a clear idea of the potential of the column to be applied to the studied samples. In spite of this, it is common that further optimization or gradient tweaks are needed once the system is run in LC × LC mode.

Once the individual conditions were selected for each dimension, the HILIC × RP method was implemented. To do that, the same grape sample used during optimization (W10) was injected into the system. The modulation time employed in the switching valve was 1.5 min and it was equipped with two identical 50 μL sampling loops. Taking into consideration the optimum flow rate determined in the ^{1}D (25 µL min^{-1}), each transfer filled 75% of the total volume available in the loops, assuring that loss of sample was not produced. The separation obtained after coupling and minor adjusting of the ^{2}D gradient profile is shown in Fig. 1A. As it can be observed, although the separation of a good number of components was obtained, very intense peaks were eluted grouped

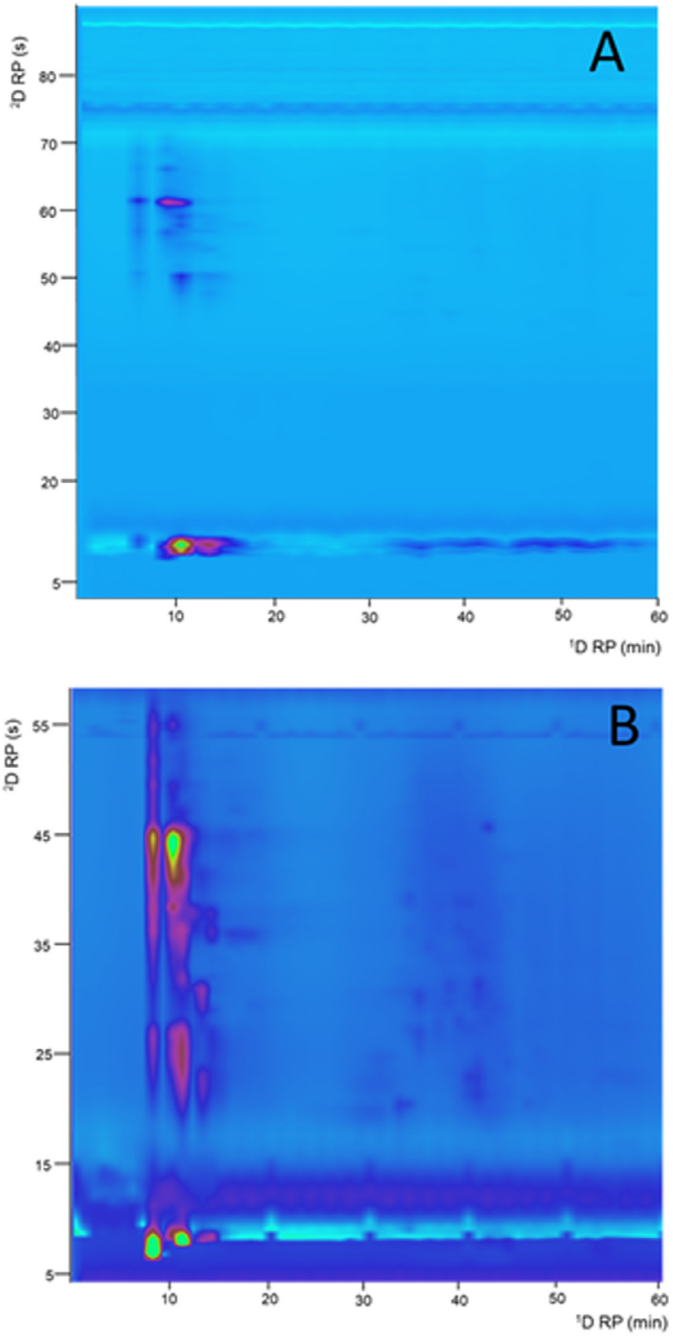

Fig. 1. 2D plots (280 nm) obtained for the polyphenolic profiling of a grape sample (W10) under the optimized HILIC × RP conditions using direct transfer between dimensions (A) and after the introduction of a dilution step (B). Separation conditions as explained in the text.

at the beginning of the ^{2}D separations (ca. t_R = 10 s). For this reason, it was decided that further modification of the ^{2}D gradients should be necessary to have a better utilization of the available 2D separation space.

Different gradients and modifications of the composition of the mobile phases were studied. A summary of the findings observed is illustrated in Fig. S4. However, none of the tested approaches allowed a significant improvement in the separation of this area. The elution of a high number of components at the beginning of the ^{2}D separations was most likely due to the solvent strength mismatch that typically occurs between HILIC and RP separations.

Table 1
Peak capacity and orthogonality values calculated for the separations corresponding to a grape sample (W10) under optimum LC × LC conditions.

		Without make-up flow	With make-up flow
^{1}D	$\overline{w}$ (min)	2.34	1.51
	^1n_c	27	40
	$<\beta>$	2.19	2.19
	^{1}n$_c$ corr.	17	26
^{2}D	$\overline{w}$ (s)	1.41	1.41
	^2n_c	65	43
LC x LC	Modulation time (min)	1.5	1
	^{2}Vinj (loop volume) (μL)	50	100
	Z_1	0.62	0.77
	Z_2	0.97	0.89
	Z_-	0.80	0.83
	Z_+	0.82	0.96
	A_0 (%)	63	74
	$^{2D}n_c$ theoretical	1095	1106

The problem could be minimized to some extent thanks to the fact that only 75% of the sampling loop volume was used to store and transfer the ^{1}D effluent, being the rest filled with ^{2}D mobile phase. In any case, as this solution was clearly insufficient, the introduction of a dilution step using an appropriate make-up flow was studied. In this case, an additional pump was used to reduce the overall solvent strength of each fraction transferred. The used make-up flow was composed of water. As the aim of the use of this approach is to reduce the fraction solvent strength, water is considered the most-favorable case for the subsequent RP separation in the ^{2}D. Moreover, based on previous findings, a 3:1 make-up solvent-to-fraction ratio was considered appropriate. As the ^{1}D flow rate employed was 25 mL min^{-1}, the make-up flow was introduced at 75 mL min^{-1}. Consequently, the sampling loops installed in the modulator were changed to an increased inner volume of 100 μL. By using this approach, not only the separation in the ^{2}D improved significantly, but also it was possible to carry out a re-optimization of the gradient employed to reduce to total ^{2}D analysis time to 1.0 min, which improves the undersampling effect of the ^{1}D separation. After implementation of the 1.0 min repetitive gradients into the HILIC × RP protocol, the obtained 2D separation was significantly improved, as illustrated in Fig. 1B. As it can be inferred from the comparison established in Fig. 1, the addition of the make-up flow was demonstrated to enhance the retention in the ^{2}D, avoiding the early elution and partial coelution of a great part of the transferred components (as shown in Fig. 1A).

The improvement achieved in terms of resolution and better use of the available separation space are translated into higher peak capacity values and orthogonality values when the make-up flow is employed, as can be seen in Table 1 (1106 *Vs* 1095). However, this is a good example of the limitations often encountered when using peak capacity as an estimation of the performance of the method. As can be observed, the theoretical peak capacity (not considering any correction in terms of degree of orthogonality) obtained for the optimum set-up (with make-up flow) was only marginally better than the peak capacity obtained without make-up flow. However, it is clearly visible from Fig. 1 that this latter set-up produced a significantly worse use of the available 2D space (Fig. 1A) as a result of the elution problems above commented. Nevertheless, the higher gradient time available when make-up flow was not employed (modulation time 1.5 min) compared to the optimum set-up (modulation time 1.0 min) as well as the fact that a lot of peaks coeluted in a narrow band around ^2t_R = 10 s caused that the ^2n_c value was higher under non-optimum conditions (Table 1). Overall, these results demonstrate how, although peak capacity may be a useful parameter to compare the performance of 2DLC methods, these values should not be considered alone when describing the figures-of-merit of the analytical approach, as they can led to a clear misjudgment.

3.2. Characterization of the polyphenolic fraction of grapes and wine

Once the HILIC × RP method was optimized, it was applied to the analysis of 10 grape samples of different maturation degree (week 1 to week 10), as well as to the analysis of the wine prepared from the samples harvested at week 9. Thanks to the application of this novel method, the evolution of the polyphenols present in the samples during grape maturation could be followed, as well as their transformation as a result of the winemaking procedure. To assign the separated compounds, the information provided by the DAD as well as the MS and MS/MS characteristic fragmentation patterns was used, and compared to the values found in the literature.

Table 2 summarizes the information collected for each peak, as well as the tentative identification reached for the wine sample. Besides, Fig. 2 shows the 2D contour plot obtained for the phenolic profile present in the wine. As it can be observed at first sight comparing Figs. 2 and 1B, the overall phenolic composition in the wine was significantly more complex than the one present in the grape samples.

Most of the detected phenolic compounds belonged to anthocyanins. As it can be observed in the 2D plot shown in Fig. 2, the separation obtained was clearly formed by two groups of components. The first one, eluting earlier from the ^{1}D was mainly composed of the anthocyanins, whereas the second group, eluting from 30 min comprised other phenolic compounds. Among anthocyanins, malvidin derivatives were the most abundant. Different malvidin-hexoside derivatives were detected thanks to their characteristic molecular $[M]^+$ ions at *m/z* 493.7 that provided a specific product ion at *m/z* 331 corresponding to the aglycone, after the neutral loss of the sugar moiety ($[M-162]^+$). Fig. 2 also shows the typical MS and MS/MS spectra for this kind of compounds (peak 10). The same fragmentation pattern was observed for malvidin-coumarylhexoside and malvidin-acetylhexoside. Apart from malvidin, other anthocyanins corresponding to delphinidin-hexoside (peaks 17 and 40) and to peonidin-6-coumaroylhexoside (peak 22) were also tentatively assigned, thanks to the detection of their typical molecular ions and the appearance of fragments compatible with their corresponding aglycones upon fragmentation.

The polyphenolic composition was also composed of vitisin A and p-coumaroyl vitisin A (peaks 29 and 25, respectively), with molecular ions at *m/z* 561.2 and 707.4, respectively. In these cases, the occurrence of fragment ions at *m/z* 399 ($[M-162]^+$ and ($[M-162-146]^+$, respectively) allowed the peaks' assignment, in agreement with those fragments reported in the literature [29]. The remaining tentatively identified compounds were flavan-3-ols. The 2D separation allowed grouping this family of compounds in the medium-last part of the analysis. In this group, diverse procyanidin dimers and trimers were detected. As can be observed in Table 2, the fragment ions detected matched the expected fragmentation pattern for both dimers (*m/z* 579) and trimers (*m/z* 867). Specifically, two peaks corresponding to procyanidin dimers were detected (peaks 23 and 32), and assigned thanks to the detection of their molecular ions as $[M+H]^+$ together with fragment ions at *m/z* 427 and 409 generated thorough a retro Diels-Alder fission and its loss of water, respectively [30], as well as a fragment corresponding to the flavan-3-ol monomer (*m/z* 291). In turn, peaks 33, 34 and 38 presented a $[M+H]^+$ ion at *m/z* 867.1. The fragmentation pattern obtained was compatible with that of procyanidin trimers. In fact, fragment ions at *m/z* 715 were present, as a result of a retro Diels-Alder fission of the heterocyclic ring, as well as others at *m/z* 579 resulting from the quinone methide cleavage of the interflavonoid bond (Fig. 2) [30].

Table 2
Identification parameters of phenolic compounds determined by LC x LC-DAD-MS/MS using the optimized HILIC × RP method.

Peak	Total t_R (min)	t_R ^{2}D (s)	λ abs	$[M + H]^+/M^+$	Main fragments	Proposed identification
1	6.13	7.60	280, 530	495.3	332	NI
2	6.41	24.55	276, 526	493.7	331	Malvidin-O-hexoside
3	6.56	35.55	286, 530	535.7	331	Malvidin-O-acetylhexoside
4	6.63	38.20	290, 530	581.6	547, 419, 401, 331, 293, 251	NI
5	6.73	43.95	284, 530	639.6	331	Malvidin-O- p-coumaroylhexoside
6	6.84	50.30	286, 530s	611.3	287	Cyanidin-O-dihexoside
7	8.13	8.05	276, 528	493.5	331	Malvidin-O-hexoside
8	8.26	15.75	272	535.1		Malvidin-O-acetylhexoside
9	8.39	23.50	280, 526	493.4	331	Malvidin-O-hexoside
10	8.41	24.65	280, 526	493.4	331	Malvidin-O-hexoside
11	8.44	26.40	282, 528	493.4	331	Malvidin-O-hexoside
12	8.53	31.50	292	535.1	331	Malvidin-O-acetylhexoside
13	8.60	35.85	298, 268	535.9	331	Malvidin-O-acetylhexoside
14	8.63	38.10	290			
15	8.73	43.90	284, 525	638.6	331	Malvidin-O-p-coumaroylhexoside
16	8.79	47.45	262			
17	10.15	8.70	272, 524	465.7	303	Delphinidin 3-hexoside
18	10.38	22.80	282, 300 s, 324	493.6	331	Malvidin-O-hexoside
19	10.60	36.05	260	536.1	331	Malvidin-O-acetylhexoside
				595.8	332	Malvidin dipentoside
20	10.70	41.85	284, 526	640.8	331	Malvidin-O-p-coumaroylhexoside
21	12.60	36.10	260, 356	493.2	331	Malvidin-O-hexoside
				535.6	331	Malvidin-O-acetylhexoside
22	29.50	30.15	275, 325s	609.6	447, 301	Peonidin-6-coumaroylhexoside
23	33.33	20.05	278	579.3	427, 409, 291	Procyanidin dimer
24	35.52	31.25	280, 310s	501	371, 259	NI
25	38.65	38.80	304, 514	707.4	399	p-Coumaroyl vitisin A
26	44.13	8.05	280, 328 s, 530	365.5	203, 275, 347	NI
27	42.32	19.70	300 s, 328	595.5	577, 443, 427, 291, 247	(Epi)gallocathechin-(*epi*)catechin
28	42.33	20.25	280, 310	475.3	456, 311	NI
29	42.40	24.20	274, 506	561.2	399	Vitisin A
30	42.51	31.05	280	797.1	365, 617	NI
31	43.59	35.20	280, 305s	562.1	399	NI
				603.5	399	Malvidin-3-(6-acetyl)glucoside-pyruvic acid
32	44.34	20.10	280	579.2	427, 409, 291	Procyanidin dimer
33	44.38	22.70	276	867.1	579, 577, 409, 715	Procyanidin trimer
34	45.46	27.80		867.1	697, 579, 577,425	Procyanidin trimer
35	50.32	19.45	278	138.8	-	p-Hydroxybenzoic acid
36	50.49	29.25	280	493.8	331	Malvidin-O-hexoside
37	52.27	16.45	280	680.1	497, 467, 305	NI
38	52.38	22.60	278	867.2	579, 449, 409	Procyanidin trimer
39	56.35	21.00	275	428.7	409, 247, 229	NI
40	56.41	24.75	280	465.3	303	Delphinidin-hexoside

*NI, not identified; s, spectral shoulder.

Although simple monomeric flavan-3-ols were not detected in this sample, a derivative with *m/z* 595.5 and characteristic fragment ions at *m/z* 577, 433, 427 and 290 was detected, corresponding to (*epi*)gallocatechin-(*epi*)catechin dimer (peak 27). A single phenolic acid, p-hydroxybenzoic acid (peak 35) was also tentatively identified. Other compounds were also detected and are summarized in Table 2, although an identification could not be reached.

3.3. Evolution of grape polyphenols during ripening

In this work, besides the optimization of a HILIC × RP method for the characterization of the phenolic profile of grapes and wine, the use of the enhanced separation power achieved by this new method was used as a direct application in a food quality strategy consisted of the study of grape anthocyanidins evolution along the post-harvest ripening stages. The phenolic profile clearly evolved with the advancement of the degree of ripeness of the grapes (W1 to W10), as shown in the 2D plots of Fig. S5. As above mentioned, anthocyanins were the main compounds detected in grape and wine samples. This fact can be seen in Fig. 3, which shows the DAD 2D plots of the sample W9 acquired at 280 nm (common wavelength for phenolic compounds) and 520 nm (specific wavelength for anthocyanins). Thanks to the specificity of 520 nm for the detection of anthocyanins, it is possible to distinguish the anthocyanins from the rest of the phenolic compounds. In this way, it is clear that the anthocyanins were grouped in the first 20 min of the analysis with a much higher intensity than the rest of the separated phenolic compounds. For this reason, the evolution of the main anthocyanins was evaluated during the ripening of the grapes using the peak volume obtained in DAD.

The identification of the selected anthocyanins can be observed in Table S2, whereas the assignment of each peak is shown in Fig. S5. Fig. 4 graphically shows the evolution of the individual anthocyanins and the behavior of each of them along the 10 weeks. Interestingly, most of the anthocyanins showed a similar trend; their initial content is low (especially at W1 and W2) and then grows to a maximum at W5-W6, followed by a decrease of these compounds from week 7 and stabilization in weeks 9 and 10. These results agree with the outcomes reported by Blancquaert *et al.* [31] who showed a maximum anthocyanin concentration at the berries state which corresponds to the period between the veraison and the maturation of the fruit which can last five to eight weeks depending on the variety and climatological

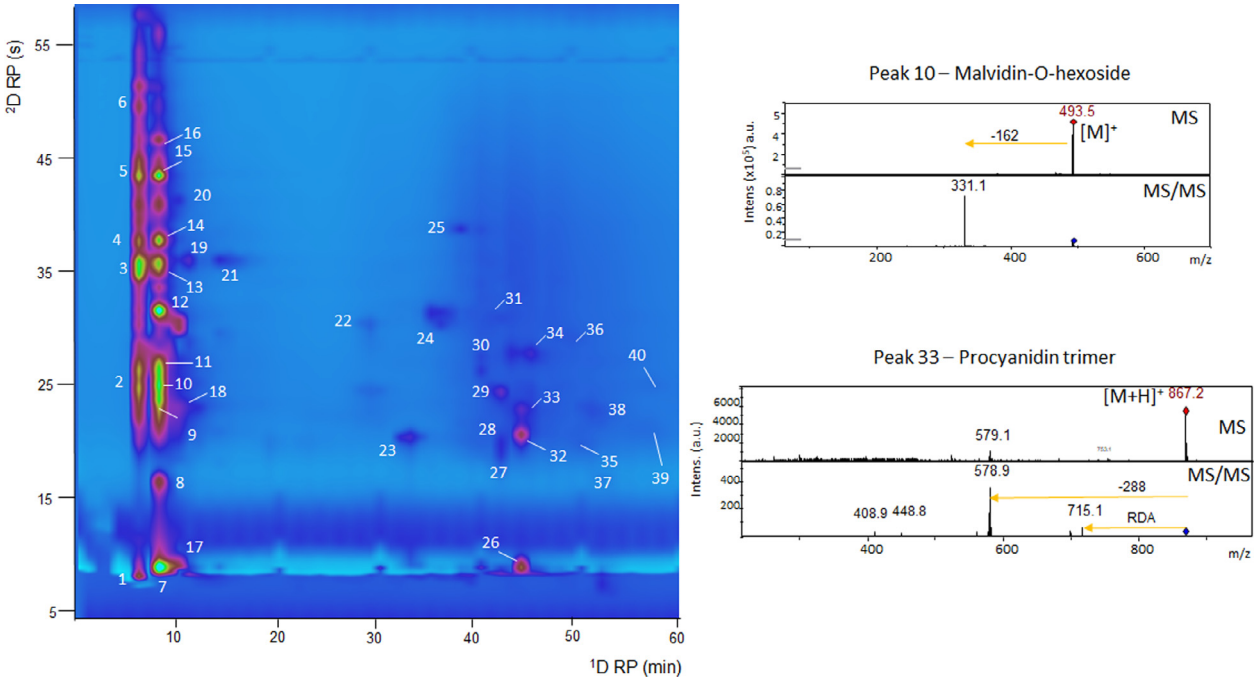

Fig. 2. Two-dimensional HILIC × RP plot (280 nm) corresponding to the Malbec wine sample analyzed under optimum conditions with the addition of make-up flow during the modulation. For peak identification, see Table 2. For detailed separation conditions, see text.

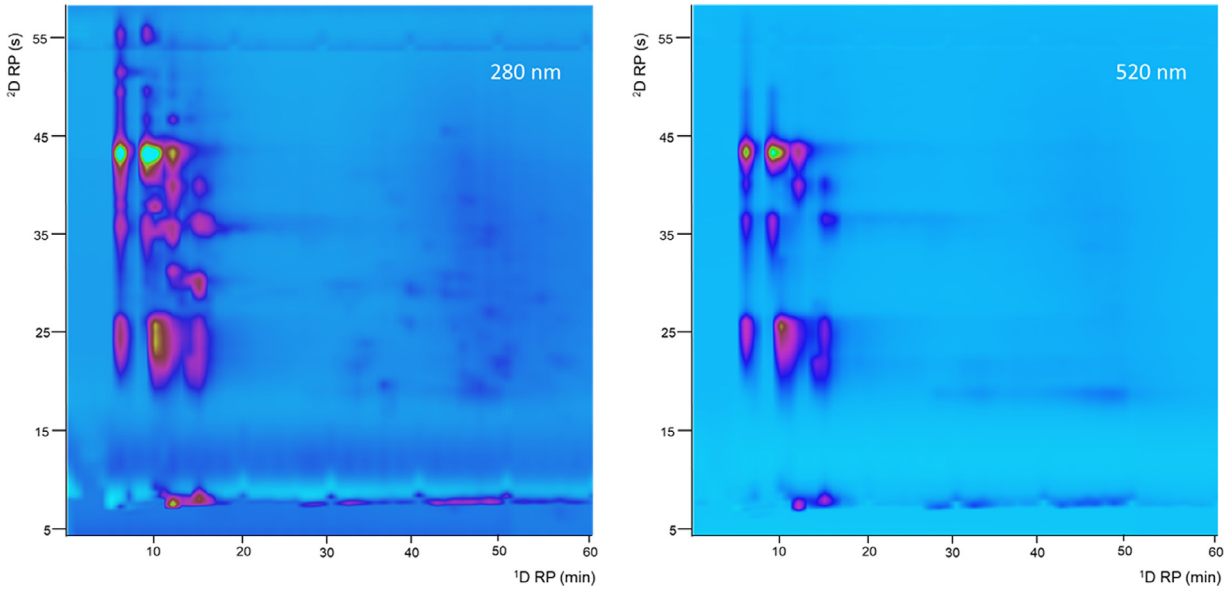

Fig. 3. 2D plots at 280 nm and 520 nm obtained under the optimum HILIC × RP separation conditions for the grape sample W9 with the addition of make-up flow during the modulation. Separation conditions as in Fig. 2.

conditions. This period characterized by the maximum concentration of anthocyanins in grapes also matches the higher concentration of sugars in the berry, known as sugar ripeness and in consequence, phenolic ripeness. This fact is due to sugars may regulate the synthesis pathways of these phenolic compounds [31].

The reduction of the anthocyanidin content after the seventh week of ripeness may be related to degradation reactions of anthocyanins in advanced stages that occur due to the exposure of grapes to high temperatures, as observed in tropical viticulture regions [32]. Therefore, considering the high anthocyanin content and its relationship with the higher sugar content in the grapes, the elaboration of wines from grapes harvested in week 6 might be advantageous for the wine quality, since the higher concentration of anthocyanins is related to greater color intensity, as well as greater color stability during wine storage. Moreover, sugar content is related to the quality of the fermentation, although other parameters related to fruit ripeness may strongly impact on the selection of the harvest time like the presence and concentration of tannins or aroma compounds like acetate esters, aldehydes or alcohols [33].

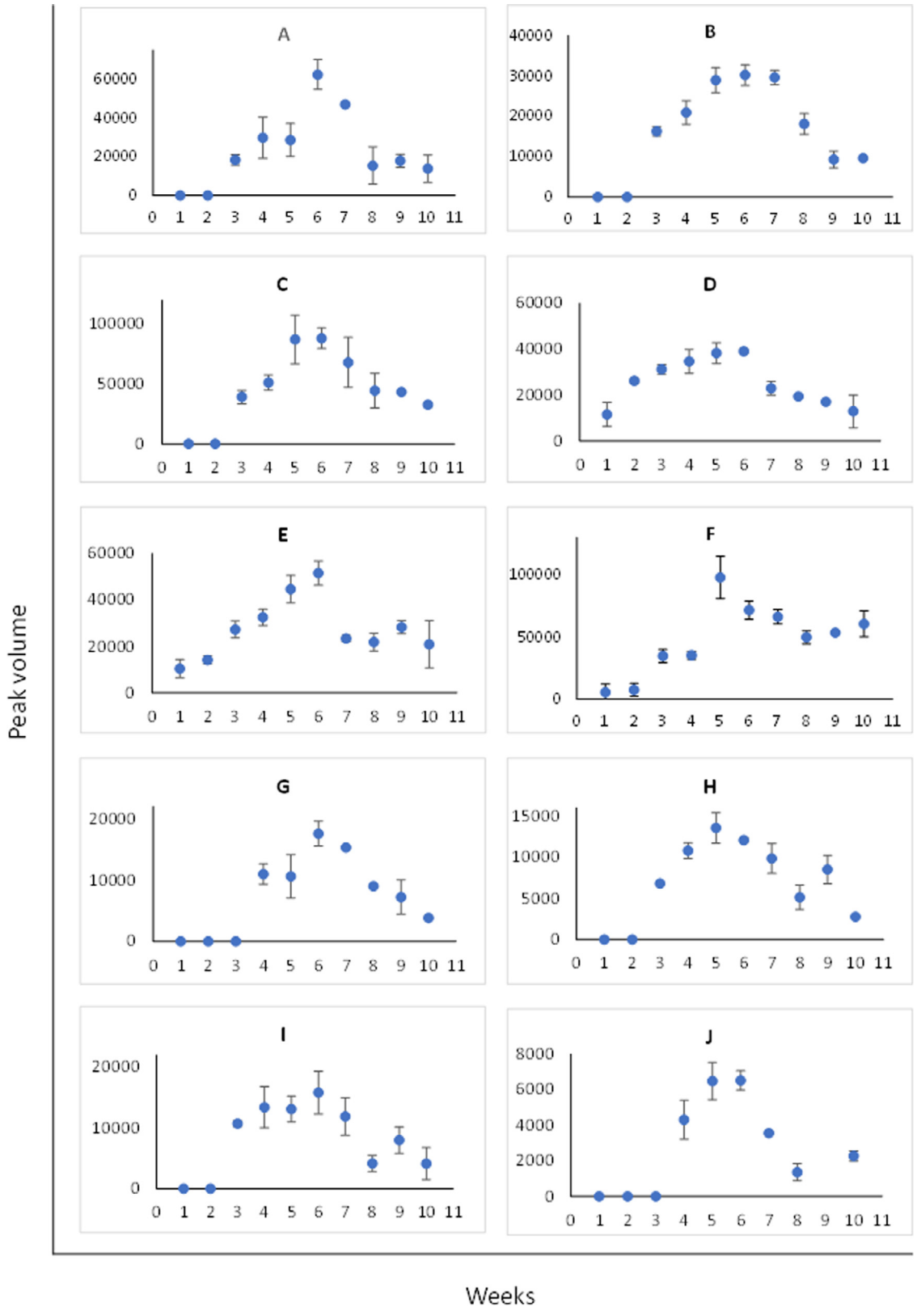

Fig. 4. Concentration trend of the main anthocyanins found during grape ripening over a period of 10 weeks (W1-W10). IDs of each graph (A-J) correspond to the identified compounds represented in Fig. S5 and Table S2.

4. Conclusions

The optimization of a new HILIC × RP method coupled to DAD and MS detectors has allowed obtaining the phenolic profiles of different grape samples involving diverse ripeness degree as well as of the wine derived from them. Different stationary and mobile phases and gradients have been tested in both dimensions, and diverse modulation procedures have been evaluated. Moreover, the final analytical conditions after final columns combination selection were also re-optimized and fine-tuned. The new method provided with a resolving power significantly enhanced compared to conventional one-dimensional approaches. Thanks to the combination of both used detectors, a good number of characteristic anthocyanins and flavan-3-ols have been tentatively identified in the wine. Most of the detected anthocyanins were composed of malvidin derivatives, being this aglycone the most abundant compound in the wine sample. Moreover, the method was useful to acquire the specific trends followed by selected polyphenols during grape ripening along 10 weeks. Results showed that anthocyanins tend to accumulate during the first 5–6 studied weeks, and then their concentration decrease towards weeks 9–10 of ripening. These findings helped define the ideal period for harvesting Malbec grapes grown in a tropical viticulture region in order to take advantage of the greater potential of anthocyanins that impart color to wines.

Overall, this methodology further demonstrates how the application of LC × LC can be a valuable tool for the analysis of very complex food samples in spite of the obvious higher complexity compared to one-dimensional methods.

Declaration of Competing Interest

The authors declare the following financial interests/personal relationships which may be considered as potential competing interests:

Miguel Herrero reports financial support was provided by Spain Ministry of Science and Innovation.

CRediT authorship contribution statement

Laura Oliveira Lago: Investigation, Methodology, Writing – original draft. **Pawel Swit:** Investigation, Methodology, Writing – review & editing. **Mairon Moura da Silva:** Resources, Methodology. **Aline Telles Biasoto Marques:** Resources, Methodology. **Juliane Welke:** Conceptualization, Methodology, Funding acquisition, Supervision, Writing – review & editing. **Lidia Montero:** Conceptualization, Methodology, Supervision, Writing – review & editing. **Miguel Herrero:** Conceptualization, Methodology, Funding acquisition, Supervision, Writing – original draft, Writing – review & editing.

Data availability

Data will be made available on request.

Acknowledgments

L.O.L. acknowledges a fellowship provided by the Coordination for the Improvement of Higher Education Personnel (Coordenação de Aperfeiçoamento de Pessoal de Nível Superior, CAPES). P.S. thanks the Research Excellence Initiative of the University of Silesia in Katowice for co-financing his research activities. L.M. acknowledges a "Ramon y Cajal" grant RYC2021-033148-I funded by MCIN/AEI/10.13039/501100011033 and by European Union NextGenerationEU/PRTR. This work was supported by grant PID2020-113050RB-I00 funded by MCIN/AEI/10.13039/501100011033 (Spain). Authors acknowledge Chromaleont S.r.l. for the support and assistance with ChromSquare software.

Supplementary materials

Supplementary material associated with this article can be found, in the online version, at doi:10.1016/j.chroma.2023.464131.

References

[1] P. Rodriguez-Lopez, A. Rueda-Robles, I. Borrás-Linares, R.M. Quirantes-Piné, T. Emanuelli, A. Segura-Carretero, J. Lozano-Sánchez, Grape and grape-based product polyphenols: a systematic review of health properties, bioavailability, and gut microbiota interactions, Horticulturae 8 (2022) 583, doi:10.3390/horticulturae8070583.

[2] R. Vejarano, M. Luján-Corro, Red wine and health: approaches to improve the phenolic content during winemaking, Front Nutr. 9 (2022), doi:10.3389/fnut.2022.890066.

[3] R. Gutiérrez-Escobar, M.J. Aliaño-González, E. Cantos-Villar, Wine polyphenol content and its influence on wine quality and properties: a review, Molecules 26 (2021) 718, doi:10.3390/molecules26030718.

[4] M.C. Ramos, E.P. Pérez-Álvarez, F. Peregrina, F. Martínez de Toda, Relationships between grape composition of Tempranillo variety and available soil water and water stress under different weather conditions, Sci. Hortic. 262 (2020) 109063, doi:10.1016/j.scienta.2019.109063.

[5] K. Wicht, M. Baert, M. Muller, E. Bandini, S. Schipperges, N. von Doehren, G. Desmet, A. de Villiers, F. Lynen, Comprehensive two-dimensional temperature-responsive × reversed phase liquid chromatography for the analysis of wine phenolics, Talanta 236 (2022) 122889, doi:10.1016/j.talanta.2021.122889.

[6] I. dos Santos, G. Bosman, J.L. Aleixandre-Tudo, W. du Toit, Direct quantification of red wine phenolics using fluorescence spectroscopy with chemometrics, Talanta 236 (2022) 122857, doi:10.1016/j.talanta.2021.122857.

[7] M.M. Vuolo, V.S. Lima, M.R. Maróstica Junior, Phenolic Compounds, in: Bioactive Compounds, Elsevier, 2019, pp. 33–50, doi:10.1016/B978-0-12-814774-0.00002-5.

[8] K.M. Kalili, A. de Villiers, Recent developments in the HPLC separation of phenolic compounds, J. Sep. Sci. 34 (2011) 854–876, doi:10.1002/jssc.201000811.

[9] A. de Villiers, P. Venter, H. Pasch, Recent advances and trends in the liquid-chromatography–mass spectrometry analysis of flavonoids, J. Chromatogr. A 1430 (2016) 16–78, doi:10.1016/j.chroma.2015.11.077.

[10] B.W.J. Pirok, A.F.G. Gargano, P.J. Schoenmakers, Optimizing separations in online comprehensive two-dimensional liquid chromatography, J. Sep. Sci. 41 (2018) 68–98, doi:10.1002/jssc.201700863.

[11] L. Montero, M. Herrero, Two-dimensional liquid chromatography approaches in Foodomics – a review, Anal. Chim. Acta 1083 (2019) 1–18, doi:10.1016/j.aca.2019.07.036.

[12] L. Montero, M. Herrero, Two dimensional liquid chromatography approaches for food authenticity, Curr. Opin. Food Sci. (2023) In press.

[13] F. Cacciola, P. Dugo, L. Mondello, Multidimensional liquid chromatography in food analysis, TrAC Trend. Analyt. Chem. 96 (2017) 116–123, doi:10.1016/j.trac.2017.06.009.

[14] P. Donato, F. Rigano, F. Cacciola, M. Schure, S. Farnetti, M. Russo, P. Dugo, L. Mondello, Comprehensive two-dimensional liquid chromatography–tandem mass spectrometry for the simultaneous determination of wine polyphenols and target contaminants, J. Chromatogr. A 1458 (2016) 54–62, doi:10.1016/j.chroma.2016.06.042.

[15] P. Dugo, F. Cacciola, P. Donato, D. Airado-Rodríguez, M. Herrero, L. Mondello, Comprehensive two-dimensional liquid chromatography to quantify polyphenols in red wines, J. Chromatogr. A 1216 (2009) 7483–7487, doi:10.1016/j.chroma.2009.04.001.

[16] M. Muller, A.G.J. Tredoux, A. de Villiers, Application of kinetically optimised online HILIC × RP-LC methods hyphenated to high resolution MS for the analysis of natural phenolics, Chromatographia 82 (2019) 181–196, doi:10.1007/s10337-018-3662-6.

[17] A.A. Aly, T. Górecki, Green comprehensive two-dimensional liquid chromatography (LC × LC) for the analysis of phenolic compounds in grape juices and wine, Anal. Bioanal. Chem. (2022), doi:10.1007/s00216-022-04241-x.

[18] L. Montero, M. Herrero, M. Prodanov, E. Ibáñez, A. Cifuentes, Characterization of grape seed procyanidins by comprehensive two-dimensional hydrophilic interaction × reversed phase liquid chromatography coupled to diode array detection and tandem mass spectrometry, Anal. Bioanal. Chem. 405 (2013) 4627–4638, doi:10.1007/s00216-012-6567-5.

[19] L. Montero, V. Sáez, D. von Baer, A. Cifuentes, M. Herrero, Profiling of Vitis vinifera L. canes (poly)phenolic compounds using comprehensive two-dimensional liquid chromatography, J. Chromatogr. A 1536 (2018) 205–215, doi:10.1016/j.chroma.2017.06.013.

[20] L. Montero, M. Herrero, E. Ibáñez, A. Cifuentes, Profiling of phenolic compounds from different apple varieties using comprehensive two-dimensional liquid chromatography, J. Chromatogr. A 1313 (2013) 275–283, doi:10.1016/j.chroma.2013.06.015.

[21] F. Cacciola, S. Farnetti, P. Dugo, P.J. Marriott, L. Mondello, Comprehensive two-dimensional liquid chromatography for polyphenol analysis in foodstuffs, J. Sep. Sci. 40 (2017) 7–24, doi:10.1002/jssc.201600704.
[22] L. Montero, E. Ibáñez, M. Russo, L. Rastrelli, A. Cifuentes, M. Herrero, Focusing and non-focusing modulation strategies for the improvement of on-line two-dimensional hydrophilic interaction chromatography × reversed phase profiling of complex food samples, Anal. Chim. Acta 985 (2017) 202–212, doi:10.1016/j.aca.2017.07.013.
[23] Y. Chen, L. Montero, J. Luo, J. Li, O.J. Schmitz, Application of the new at-column dilution (ACD) modulator for the two-dimensional RP×HILIC analysis of Buddleja davidii, Anal Bioanal Chem 412 (2020) 1483–1495, doi:10.1007/s00216-020-02392-3.
[24] B.G. COOMBE, Growth Stages of the Grapevine: adoption of a system for identifying grapevine growth stages, Aust. J. Grape Wine Res. 1 (1995) 104–110, doi:10.1111/j.1755-0238.1995.tb00086.x.
[25] E. Rodrigues, L.R.B. Mariutti, A.Z. Mercadante, Carotenoids and phenolic compounds from *Solanum sessiliflorum*, an unexploited Amazonian fruit, and their scavenging capacities against reactive oxygen and nitrogen species, J. Agric. Food Chem. 61 (2013) 3022–3029, doi:10.1021/jf3054214.
[26] M. Camenzuli, P.J. Schoenmakers, A new measure of orthogonality for multi-dimensional chromatography, Anal. Chim. Acta 838 (2014) 93–101, doi:10.1016/j.aca.2014.05.048.
[27] R. Flamini, M. De Rosso, L. Bavaresco, Study of grape polyphenols by liquid chromatography-high-resolution mass spectrometry (UHPLC/QTOF) and suspect screening analysis, J. Anal. Method. Chem. 2015 (2015) 1–10, doi:10.1155/2015/350259.
[28] J. Yang, T.E. Martinson, R.H. Liu, Phytochemical profiles and antioxidant activities of wine grapes, Food Chem. 116 (2009) 332–339, doi:10.1016/j.foodchem.2009.02.021.
[29] R. Flamini, Recent applications of mass spectrometry in the study of grape and wine polyphenols, ISRN Spectrosc. 2013 (2013) 1–45, doi:10.1155/2013/813563.
[30] E.A. Rue, M.D. Rush, R.B. van Breemen, Procyanidins: a comprehensive review encompassing structure elucidation via mass spectrometry, Phytochem. Rev. 17 (2018) 1–16, doi:10.1007/s11101-017-9507-3.
[31] E.H. Blancquaert, A. Oberholster, J.M. Ricardo-da-Silva, A.J. Deloire, Grape flavonoid evolution and composition under altered light and temperature conditions in cabernet sauvignon (Vitis vinifera L.), Front Plant Sci. 10 (2019), doi:10.3389/fpls.2019.01062.
[32] N. Torres, J. Martínez-Lüscher, E. Porte, S.K. Kurtural, Optimal ranges and thresholds of grape berry solar radiation for flavonoid biosynthesis in warm climates, Front. Plant Sci. 11 (2020), doi:10.3389/fpls.2020.00931.
[33] K. Bindon, C. Varela, J. Kennedy, H. Holt, M. Herderich, Relationships between harvest time and wine composition in Vitis vinifera L. cv. Cabernet Sauvignon 1. Grape and wine chemistry, Food Chem. 138 (2013) 1696–1705, doi:10.1016/j.foodchem.2012.09.146.